International Journal of Mechanical, Industrial and Aerospace Sciences
ISSN: 2517-9950
Vol:6, No:2, 2012

Port Positions on the Mixing Efficiency of a Rotor-Type Mixer – A Numerical Study

Y. C. Liou, J. M. Miao, T. L. Liu, and M. H. Ho

***Abstract*—**The purpose of this study was to explore the complex flow structure a novel active-type micromixer that based on concept of Wankle-type rotor. The characteristics of this micromixer are two folds; a rapid mixing of reagents in a limited space due to the generation of multiple vortices and a graduate increment in dynamic pressure as the mixed reagents is delivered to the output ports.

Present micro-mixer is consisted of a rotor with shape of triangle column, a blending chamber and several inlet and outlet ports. The geometry of blending chamber is designed to make the rotor can be freely internal rotated with a constant eccentricity ratio. When the shape of the blending chamber and the rotor are fixed, the effects of rotating speed of rotor and the relative locations of ports on the mixing efficiency are numerical studied. The governing equations are unsteady, two-dimensional incompressible Navier-Stokes equation and the working fluid is the water. The species concentration equation is also solved to reveal the mass transfer process of reagents in various regions then to evaluate the mixing efficiency.

The dynamic mesh technique was implemented to model the dynamic volume shrinkage and expansion of three individual sub-regions of blending chamber when the rotor conducted a complete rotating cycle. Six types of ports configuration on the mixing efficiency are considered in a range of Reynolds number from 10 to 300. The rapid mixing process was accomplished with the multiple vortex structures within a tiny space due to the equilibrium of shear force, viscous force and inertial force. Results showed that the highest mixing efficiency could be attained in the following conditions: two inlet and two outlet ports configuration, that is an included angle of 60 degrees between two inlets and an included angle of 120 degrees between inlet and outlet ports when Re=10.

***Keywords*—**active micro-mixer, CFD, mixing efficiency, ports configuration, Reynolds number, Wankle-type rotor

I. Introduction

THE micro-mixer is the key component is the micro-fluidics or μ-TAS. The characteristics of a micro-mixer include small in size, less samplings required, fast reaction time, reduced experimental errors caused by manual operation, increased overall system stability, reduced sample consumption and shortened testing time.

Yi-Chun Liou is with the School of Defense Science Studies, Chung Cheng Institute of Technology, National Defense University , Taiwan, R.O.C (e-mail: valky_liu@hotmail.com.tw).

Jr-Ming Miao is with the Department of Biomechatronics Engineering, National Pingtung University of Science and Technology, Taiwan, R.O.C (corresponding author to provide phone: +886-8-7703202#7566;e-mail: jmmiao@mail.npust.edu.tw).

Tsung-Long Liu is with the Department of Power Vehicle and System Engineering, Chung Cheng Institute of technology, National Defense University, Taiwan, R.O.C (e-mail: tlliu@ndu.edu.tw).

Ming-Hui Ho is with the Department of Biomechatronics Engineering, National Pingtung University of Science and Technology, Taiwan, R.O.C (corresponding author to provide phone: +886-8-7703202#7464;e-mail: kandyho@yahoo.com).

Besides, a micro-mixer is easy to operate and convenient to carry around, and its light structure can substantially bring down the manufacturing cost. Judging from the development towards integrated analytical system on a chip, the development of high-efficiency micro-mixers would have a great influence on chemistry and biotechnology fields.

With the increased demand for faster reaction in chemical micro-plant engineering technology and bio-technology over recent years, the requirements for micro-mixers' minimization and less sample volume have now become more pressing. Consequently, the trend in micro-mixers design and application is not only to less damage in environment but also to user friendly. This is the reason why Kim *et al*. [1] proposed of a novel active-type micro-mixer device with a rotor is so imperative in 2009.

According to report of Liu *et al*. [2] and Nguyen [3], micro-mixers nowadays can be categorized into passive micro-mixers, and active micro-mixers, shown in Fig. 1. Typically, a special wall structure is used in a passive micro-mixer to destroy the laminar flow structure in micro-channels becomes a chaotic convection effect when the fluids flow through the structure or increase the contact area between fluid streams, thereby speeding up the mixing of different fluid streams. The methods include Y-shaped and T-shaped channels, multi-layer channels, the split and re-combination of fluids, chaotic mixing, jet flow collision mixing, re-circulating flow mixers and others. On the part of an active micromixer, either a movable component is added to the system or a stirring force is exerted from outside in the mixing process. Those external forces can be induced from pressure gradient, temperature gradient, the driving force of an electric field, the driving force of a magnetic field, heat convection, ultrasound, etc.

Compared with passive micro-mixers, active micro-mixers have the advantages of less reaction sample and space required, shorter mixing time and easy to control. However, they have their own drawbacks, for example additional movable components are required such as rotors, stirrers, helixes, etc. Besides, an active micro-mixer is much more difficult to manufacture or proper assemble. In spite of those un-convinces, active micro-mixers have their strength in terms of biomedicine technology such as higher mixing efficiency for fluids in micro-channels, fast screening of test samples and reagents as well as minimization of medical equipment. In a traditional design, an active micro-mixer usually uses electricity, magnet, heat or sound wave to drive the mixing process of reactants and reagents. However, it is possible to change the nature of reactants and reagents in mixing process such as the stretch or

breakup of red blood cell in the biochip. It has necessitated that the design of a new micro-rotor mixer in biochip system to advance chemical reaction. Therefore, we planned to design a novel rotor-type micromixer and to explore the mixing mechanism with CFD method.

II. The Theory and Mechanism of a Micro-Mixer

The mixing of two or more different fluids mainly depends on the effect of molecular diffusion, which is in direct proportion to (1) fluid's gradient of mole concentration and (2) interfacial surface areas between fluids. Consequently, the addition of a blending mechanism in a flow field can create turbulence and increase interfacial surface area, thereby expanding molecular diffusion and leading to a rapid mixing. However, when flow channels are shrunk to as small as hundreds of μm scale, the Reynolds numbers with the channel hydraulic diameter as the characteristic length usually ranged between 0.01 and 100. In this region, the fluid fields in the channels are belonging to laminar flow, which makes it extremely difficult to enhance mixing efficiency by producing turbulences. Hence, how to effective increase interfacial surface area between two fluids in a laminar flow by using some active mechanisms has become an important task for the current micro-mixer-related studies. Below are the three requirements put forth by Miyake *et al*. [4] that a micro-mixer should meet:

(a) be capable of mixing with a very small amount of fluids (approx. 1 μl)
(b) be capable of using a simple method to achieve a fast and even mixing
(c) simple and easy to be produced.

The most important purpose for a mixer is to generate cyclical, alternate, transverse flow structures from hydrodynamic point of view. To achieve this, different flow channels and wall structures are designed and tested in the past ten years. Among them, SHM (Staggered Herringbone Mixer) presented by Stroock [5] and BEM (Barrier Embedded Micromixer) by Kim [6] are the most representative designs. The latest designs of passive mixers make use of various flow channels to handle 3D flow fields when the Reynolds number is higher than 1. Examples include the design put forward by Cortes-Quiroz *et al*. [7], in which a fin-shaped baffle is added in flow channels to improve mixing efficiency; the one presented by Ansari *et al*. [8], where imbalanced flow channels and method of collision are adopted to increase mixing efficiency, and the design raised by Lin *et al*. [9], in which a square-wave structure and a cyclical cubic groove are combined to strengthen mixing effect. On the other hand, active micro-mixers also have some strength. For examples, flows and mixing can be controlled at the same time to enable two or more fluids to reach an ideal mixing in a limited space within a very short time.

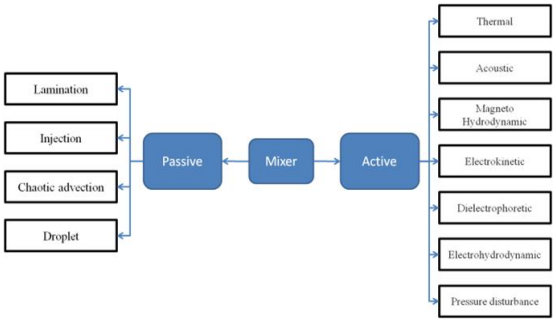

Fig. 1 The mixer classification chart [3]

III. Current Development and Application of Micro-Mixers

The micro-mixer presented by Meijer *et al*. [10] adopted an stirring artificial cilium in a very small space to produce cross-interaction effect. They intended to destroy laminar flows and produce vortex envelopes, thereby to speed up the mixing of two or more fluids using a theory similar to that of a micro-mixer. This observation proves that the production of vortex envelopes can increase mixing efficiency. The ultrasonic micro-mixer put forth by Yang *et al*. [11-12] added a PZT piezoelectric material (5mm x 4mm x 0.15mm) to generate ultrasonic vibration wave using to achieve the purpose of mixing.

Li *et al*. [13] used T-junction microchannels as basic components for a mixer and added cyclical pulsating flows with phase difference of 180° to the fluids at inlets to consider the mixing performance. The results showed cyclical pulsating flows could enable the two fluids to enter the mixer in an alternate manner to further produce a stretching and expanding effect on the interfacial surface of the fluids along the channel direction and result in a better mixing performance. Hsu [14] used numerical simulation to find out how to use a microchannel mixer with a simple geometric structure and the method of cyclical inflow (active) to improve mixing efficiency. It was found that for cyclical pulsating flows under active control, the design of phase difference between streams had a great influence on mixing efficiency, and improper application of phase angle might produce a negative effect on mixing efficiency.

Chang [15] successfully combined the functions of both active and passive micromixers by making use of the simple characteristics of passive micro-mixers and magnetized nano-fluids as working fluid. The mixer was characterized by its controllability, and when a magnetic field was applied, it could produce an effect similar to the rotation or jostling of magnetic rods, thereby enhancing its mixing effect. The results of the experiment showed that when the magnetic fluid was under the certain thread value of a magnetic field, the fluid would flow downstream and lead to a more even mixing due to diffusion effect. For fluids of the same concentration and with the same distance from the center, the stronger the magnetic field, the more even the mixing, and when the magnetic field was the same, the mixing would become more even with the increase of concentration of magnetic fluid. Wu *et al*. [16] used

micro-PIV system to visualize and reconstruct the complex flow fields with a active micro-mixer under operation. To make an active micro-mixer, they first made A1 film to deposit on a piece of glass and conducted lithography manufacturing process before using aluminum-erosion liquid to etch out a resistance heater. After that, the heater was put in ICP together with a PDMS microchannel for a change into surface treatment and then combined them together. Their experimental results found that in a microchannel in flow pattern of a laminar flow (with a low Reynolds number), the addition of active pulsating flows could substantially improve its mixing effect.

The published literature contains none of studies about the unsteady flow behavior of a Wankle-type micromixer executing cycling motion of rotor. Consequently, the objective of present work is to investigate the multiple vortex structure generated by the eccentrically dynamic motion of rotor under different rotating speed and inflow Reynolds number. Four configurations of inlet/outlet ports location are tested and intended to find out the optimum combination of operational parameters on generation of maximum mixing efficiency over a complete cycle. Vorticity contours over a complete cycle of rotor motion are plotted to explain the unsteady flow mechanisms generating the maximum mixing efficiency

IV. Research Method

A. Governing Equations

The working fluid is water and the flow field within the Wankle-type micromixer is governed by the unsteady and two-dimensional incompressible Navier-Stoke's equations coupled with the dynamic mesh motions to model the motion of rotor. The unsteady incompressible Navier-Stokes equations including of continuity equation and momentum equation as:

$$\left(\nabla \bullet \vec{u}\right) = 0 \tag{1}$$

$$\frac{\partial \vec{u}}{\partial t} + \left(\vec{u} \bullet \nabla\right)\vec{u} = -\frac{\nabla p}{\rho} + \upsilon \nabla^2 \vec{u} \tag{2}$$

where $\vec{u}$ is the velocity vector, p is the pressure, υ is the kinematic viscosity and ρ is the density of mixture.

The governed equations are solved by the FLUENT@ 12.1.06 software based on the control volume method. The transient, staggered pressure-based solver is employed due to the flow field is varied (especially in the three sub-regions of blending chamber) during the cyclical eccentrically dynamic motions of a rotor. In governed equations, the convection flux term is discretized with the second-order UPWIND scheme, while the diffusion flux term is discretized with the central differencing scheme. As for the coupling of velocity and the pressure in the momentum equations, the SIMPLEC (semi-implicit method for pressure-linked equations consistent) algorithm is applied. The AMG (algebraic multi-grid) scheme is also implemented for acceleration of convergence of all scalar variables during each time interval. To model the cycling motion of the rotor with various rotating speed, present study adopts the dynamic mesh technique to treat the deformation of mesh cells in computation. Thereby, the temporal grid deformation is governed by the Geometric Conservation Law (GCL) in each time interval.

When a fluid contains multiple ingredients, it is assumed that different ingredients are mixed on a molecular surface and all of them have the same temperature, pressure, velocity, etc., and that mass transfer takes place through convection and diffusion. Different ingredients are indicated with A, B, C, and so on. Concentration - C_A - stands for A's mass per unit volume. Mass fraction represents the ratio of A's mass at a certain point to all mixed mass. Hence, the equation can be expressed as below:

$$Y_A = c_A/\rho \tag{3}$$

Mass fraction is the most suitable variable for the description of the mass transfer model of convection and diffusion. The equation of convection and diffusion mass transfer can be expressed as below:

$$\frac{\partial \rho Y_A}{\partial t} + \nabla \cdot (\rho U Y_A) - \nabla \cdot (\Gamma_A \nabla Y_A) = 0 \tag{4}$$

The equation assumes that the zero source term of A neither come into existence nor vanish, and that molecule diffusion coefficient - Γ_A - is a constant.

B. Model Description and Boundary Conditions

As this study was conducted based on the simulation of a Wankle-type micromixer operation process, calculation zones within the blending chamber would change their space with rotor movement and grid distribution would also be re-adjusted accordingly at each time step. The housing shape of blending chamber was evaluated from the predetermined moving path of rotor in advance. To fully utilize the characteristics of dynamic mesh technology, it was necessary to use structuralized square grids to cover the whole mixing chamber, namely calculation zone, the purpose of which was to ensure that highly orthogonal grids could be maintained in prominent parts of a flow field, thereby to precisely grasp the characteristics of the boundary layer and observe the change of the flow field. The grid layout constructed in this study had the following features: in the application of dynamic grids technology, the rotor and the square grids covering the mixing chamber were seen as an entity, whose relative position would be re-adjusted along the moving track, and new grids would be regenerated in each time step. This enables us to obtain the changes of the variables in the mixing chamber in a precise manner. Fig. 2 is the geometric structure and the grid layout. The long axis of the rotor is 14.4mm, short axis is 10.4mm, generate radius R is 5mm, eccentric moment E is 1mm, import width is 0.625mm, export width is 1.25mm, and the gap between housing and rotor is 0.2mm.

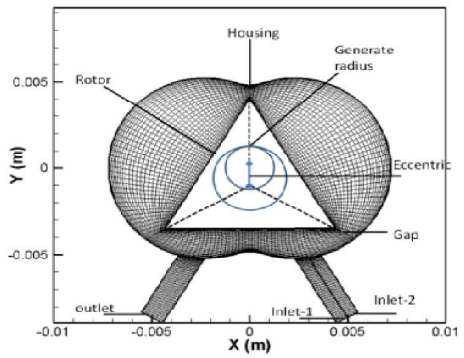

Fig. 2 The grid layout of the micro-rotor mixer

In this study, a concept from rotor-like engine structure (Wankel type) was developed to design present rotor-type micromixer. The eccentrically dynamic motion of rotor was dominated by external User Defined Functions (UDFs complied with C language program) during oscillated rotating speed. There is a small gap between the rotor and housing to avoid the lubrication problem. The inlet plane was even divided to allow the reactant and reagent flows into the blending chamber to mix. After mixing process, the combined flow streams were flaw out from the output port to downstream.

On the rotor surface the instantaneous flow velocity is set equal to the prescribed eccentrically dynamic motion. A no-slip boundary condition is imposed on the chamber and tube surfaces. The inflow (inlet port) and outflow (outlet port) boundary conditions are set as velocity inlet type and pressure outlet type in Fluent@ software respectively. The mass fraction of species is also given in the inlet velocity plane. The initial conditions for all runs are assumed as the water flow field is rest before the rotor starting to perform cycling motion. The operation pressure is 1 atm.

C. Quantification of Mixing Performance

Lee and Kwon [17], Lee *et al*. [18], Stroock *et al*. [5] and Hardt and Schönfeld [19], all came up with a general formula to quantify mixing efficiency.

$$\eta_N = \left(1 - 2 \times \sqrt{\frac{1}{A}\sum (c_i - 0.5)^2 A_i}\right) \times 100\% \quad (5)$$

The A_i in the above equation denotes the area of ith ingredient on interlacing section, c_i the mass fraction of ith ingredient, A the area of interlacing section, and η_N numerical mixing efficiency.

For computation work, the following equation proposed by Engler *et al*. [20] to define the mixing efficiency of a micro-mixer was more easily in post-processing.

$$\alpha = 1 - \sqrt{\frac{\sigma^2_{mean}}{\sigma^2_{max}}} \quad (6)$$

$$\sigma^2_{mean} = \frac{1}{n}\sum_{i=1}^{n}(c_i - c_{max})^2 \quad (7)$$

The α in the equation stands for the definition of mixing efficiency; σ_{max} represents the maximum change of mixing concentration value (which is 0.5 here); n indicates the number of grids for the concentration value on a certain cross-section; c_i is the concentration value of a certain grid; c_{max} denotes the maximum mixing concentration value (which is 0.5 here). Generally, the physical sense of calculation of mixing efficiency from equation (5) and equation (6) is the same.

V. Results and Discussion

FLUENT™, a hydrodynamics software package, was used as a numerical simulation tool in this study to analyze the mixing efficiency and the transient flow field structure of a micro-rotor mixer operating in different conditions. ANSYS ICEMCFD® was first used to build physical models and grids. Structured body-fitted grids were generated for flow field analysis. The governing equation used for flow field calculation was Navier-Stokes equations and a scalar transport equation was coupled to solve for the mass transfer between species. The port locations and flow parameters (Reynolds number, rotating speed) on the developing flow field and mixing efficiency are considered. Table 1 is the research matrix.

TABLE I
THE RESEARCH MATRIX

Case No.	Geometric structure	Reynolds Number(Re)	Angular velocity(r.p.m.)
Geo-1			
Geo-2			
Geo-3		10, 100, 300	30, 90, 150, 300
Geo-4			
Geo-5			

First of all, runs with Geo-1 model were conducted to perform the grid refinement test. The grid number of original structure was 5355, which was later multiplied by 2 and 4 times to increase grids density. Fig. 3 is the calculation results of mixing efficiency with respect to the Reynolds number, showing a better grid layout can be obtained by multiplying by 2 times from original grid distribution. As a result, a grid layout based on original grids number multiplied by 2 times was adopted for all subsequent calculations.

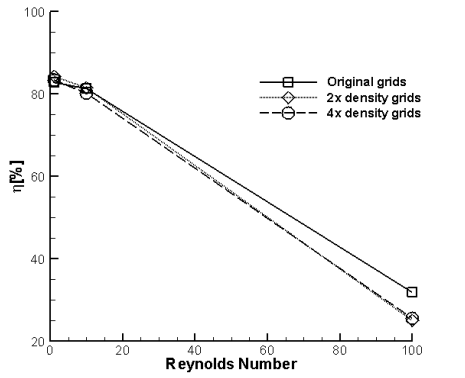

Fig. 3 The grids refinement test results

The calculation example of case Geo-1 is a model in which the divided angle between inlet and outlet port is 60 degrees, both inlet and outlet ports are located on the compression side of blending chamber and the total grid number is 10710 (as shown in Fig. 2). After the fluid flows in, it will first run into the right side of the chamber and form a small vortex flow, which will either expand or shrink depending on the angle of the rotor. When the tip of the rotor rotates to the shorter bridge of the chamber, the right side region will become narrower and function like a nozzle and form a jet flow before flowing into the outlet port [as shown in Fig. 4(a)]. However, in the flowing process, some fluid would flow directly from the inlet port into the outlet port [as shown in Fig. 4(b)]. The generation of either vortex or jet flows can effectively increase the mixing efficiency.

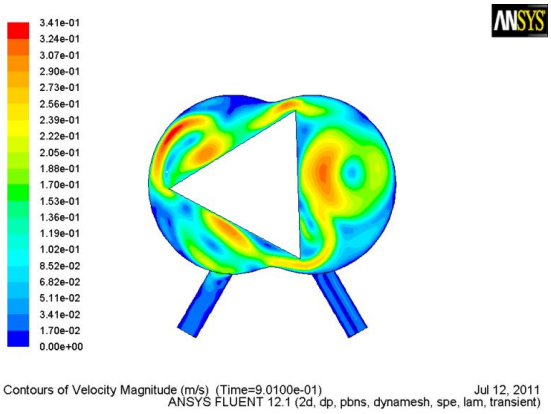

(a)

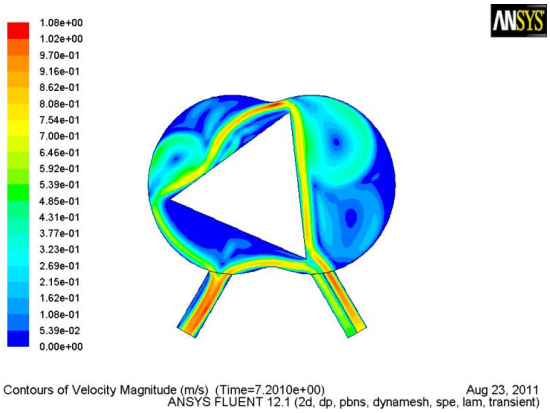

(b)

Fig. 4 The velocity contours of case Geo-1
(a)Re=10 ω = 150 r.p.m. (b)Re=300 ω = 30 r.p.m

In the calculation example of case Geo-2, the position of outlet port is changed to 120 degrees clockwise from that of the inlet port as shown in Fig. 5. After the fluids enter into the blending chamber from the inlet port, a small amount of the fluids will flow out through the outlet port at the beginning of the cycle, and the rest amount of the reagents can be fully mixed with the reactants after completing the rotation of the rotor. When condition of Re=10 and a rotation speed of 150 r.p.m. , the mixing efficiency can reach up to 85.03%. Fig. 6 is the instant velocity contours for different Reynolds number and rotating speed of rotor. A multiple vortex structure was observed. This is due to the unbalance of wall shear force from rotating rotor and inertial as viscous force from working fluid.

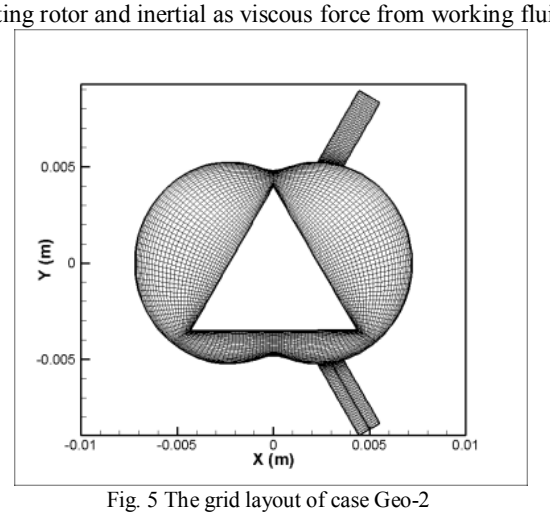

Fig. 5 The grid layout of case Geo-2

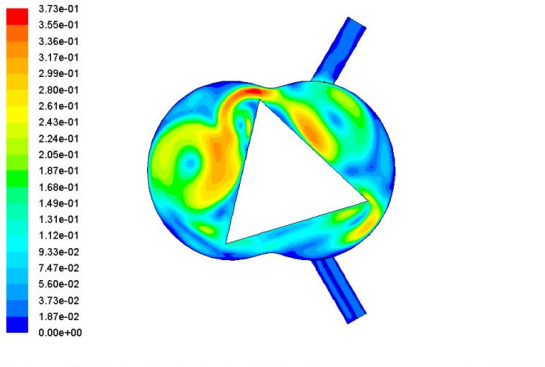

(a)

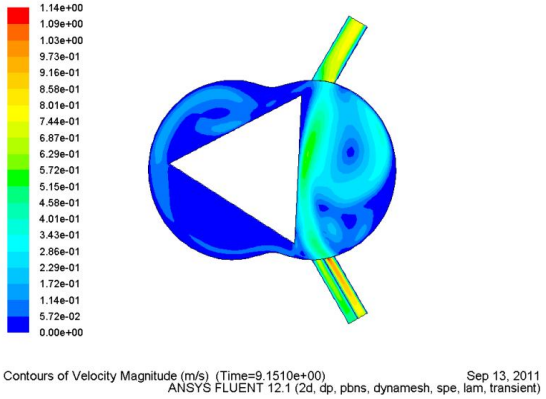

(b)

Fig. 6 The velocity contours of case Geo-2
(a)Re=10 ω = 150 r.p.m. (b)Re=300 ω = 30 r.p.m

In the calculation example of case Geo-3, the position of the outlet ports is further changed to 180 degrees from the inlet port (i.e. just opposite to the inlet port). Fig. 7 shows the grid layout. After streams entering from the inlet port, the fluids would impact the side of the rotor and form a vortex which is bigger than the scope of case Geo-1. The vortex would enlarge in the mixing chamber to sufficiently mix the reagents. When Re=300, the vortex flow would become stronger and produce a bigger vortex below the outlet port. When the rotor is continuing rotating, the open distance between the rotor and the inlet port would produce a function similar to that of a nozzle-diffuser to increase then reduce the flow speed, thereby improving the mixing efficiency as shown in Fig. 8. When Re=10 and at a rotation speed of 150 r.p.m. , the mixing efficiency could reach to 85% [as shown in Fig. 8(a)]. When Re=300 and at a rotation speed of 30 r.p.m. , the mixing efficiency could be reduced to the lowest at 23.89% [as shown in Fig. 8(b)]. When Re=10, rotation speed has no obvious influence on mixing efficiency. However, when Reynolds number is increased, the increase of rotation speed could help maintain the mixing efficiency. The reason is that before the vortex flow in the mixing chamber, it has enough time to sufficiently mix the reagents, even if some of the fluids have already been drained out of the chamber.

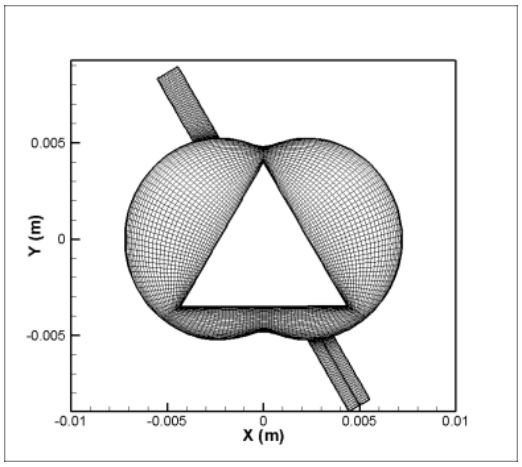

Fig. 7 The grid layout of case Geo-3

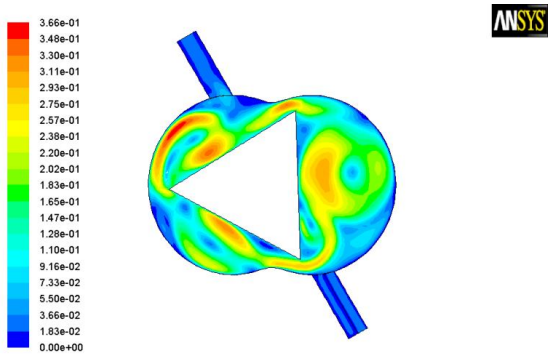

(a)

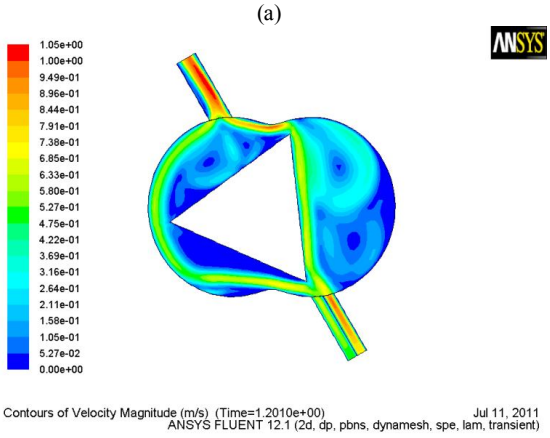

(b)

Fig. 8 The velocity contours of case Geo-3
(a)Re=10 ω = 150 r.p.m. (b)Re=300 ω = 30 r.p.m

The example of case Geo-4 is a structure with one inlet port and two outlet ports, the positions of the two outlet ports are divided to respectively 120 degrees and 180 degrees clockwise from the inlet port. Fig. 9 is the grid layout of case Geo-4. Different from case Geo-3, case Geo-4 has an additional outlet port as shown in the figure. It was found that when Re=100 and at rotation speeds of 30 and 90rpm, most of the fluid would

flow out through the outlet port on the right side of chamber (see Fig. 10). When Reynolds number is smaller than 100 and the rotor is running at 90 r.p.m. , a better mixing effect can be obtained. It may be because when at 90 r.p.m. , the flow speed at the inlet and the rotor speed happen to be able to work together to produce a vortex flow to mix the reagents, after which the fluid can immediately flow out the chamber through the outlet on the right side [see Fig. 10(b)].

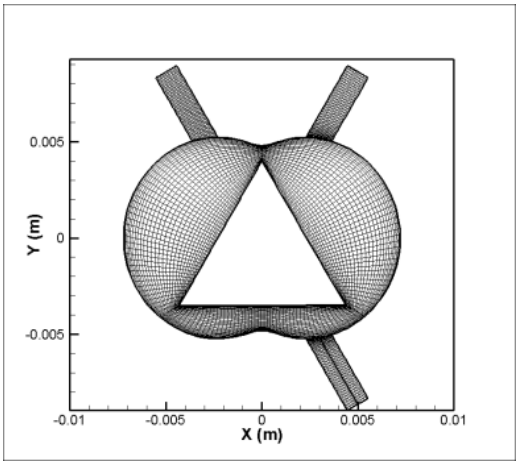

Fig. 9 The grid layout of case Geo-4

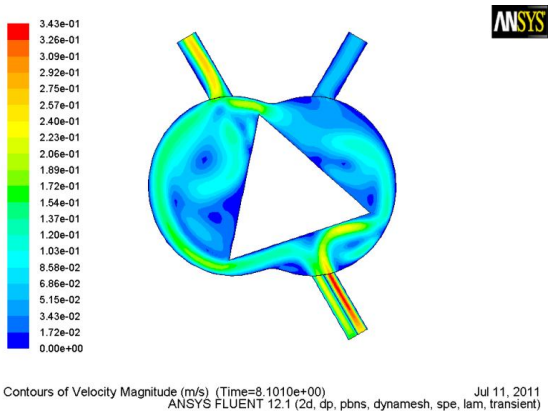

(a)

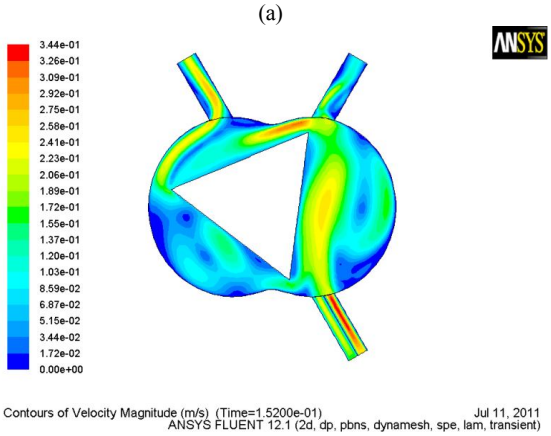

(b)

Fig. 10 The velocity contours of case Geo-4
(a)Re=100 ω = 30 r.p.m. (b)Re=100 ω = 90 r.p.m

Case Geo-5 is a structure with two inlet ports and two outlet ports. The inlets and outlets are located at the four corners of the mixing chamber. Both the divided angle between the two inlets and the one between the two outlets are 60 degrees, and the divided angle between the inlet and the outlet is 120 degrees. Fig. 11 is the grid layout of case Geo-5. After water and alcohol flow into the mixing chamber from different inlets, they are mixed together through the eccentric rotation of the rotor. In the process, a vortex flow and a local jet flow will be generated. When Re=10 and at a rotation speed of 300 r.p.m., there is no dead corner in the mixing chamber [see Fig. 12(a)]. But when Re=300, the fluid will flow out the chamber before being mixed, leading to a lower mixing efficiency [see Fig. 12(b)].

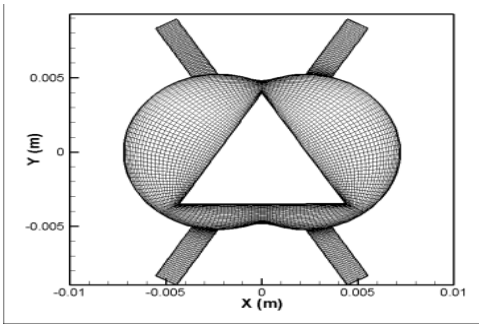

Fig. 11 The grid layout of case Geo-5

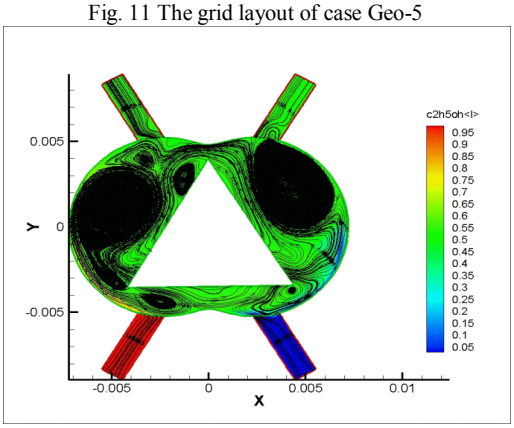

(a)

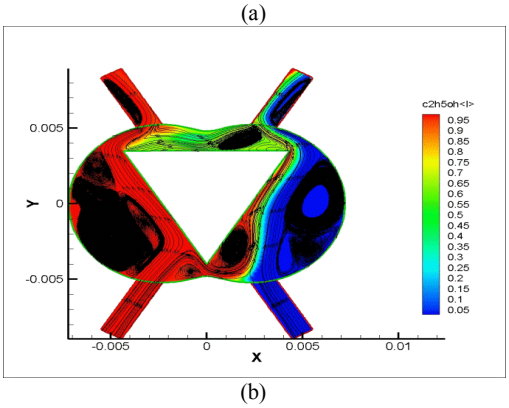

(b)

Fig. 12 The alcohol concentration contours and streamline of case Geo-5 (a)Re=10 ω = 150 r.p.m. (b)Re=300 ω = 30 r.p.m.

Fig. 13 and 14 show the quantitative analyses of relations

between inlets and outlets port number and positions, rotor rotation speed and mixing efficiency in the calculation examples of five configurations.

VI. Conclusion

Design of Wankle-type micromixer is a complex problem because of a wide range of factors influenced on the unsteady flow structures with the blending chamber. Present work employed the CFD model with dynamic mesh technique to test the effect of port locations on the mixing efficiency under various operational conditions.

Several conclusions can be stated from our numerical results.

1) A higher mixing efficiency cannot be achieved only by increasing of Reynolds number or rotation speed. A higher mixing efficiency hinges on a better combination of Reynolds number, port location and rotation speed, of which Geo-5 is the best example.
2) When there are multiple vortex flow structure in the calculation zone, after reagents flowing in the blending chamber, the fluid can interact with the vortex and results in a higher mixing efficiency. However, if the fluid velocity is too fast, i.e. high Reynolds number, the speed up of rotor is less significant.
3) When Re=10, ports configuration has no obvious influence on mixing efficiency. Moreover, a rotation speed of rotor exceeding of 90rpm can not contribute to a higher mixing efficiency in present tested range of flow parameters.
4) For all port configurations, condition of Re=10 and 30rpm for rotor is the best combination that can reach the highest mixing efficiency.
5) Among tested runs, the case Geo-5 exhibited the highest mixing efficiency at 85.88%, while the case Geo-4 has the poorest mixing efficiency at 12.54%.

It is hoped that the results of this research can serve as useful reference for the design of new rotor-based mixers in the future.

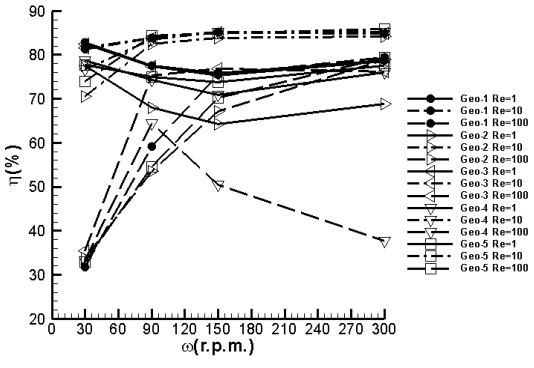

Fig. 13 A comparison of mixing efficiency under different Reynolds numbers

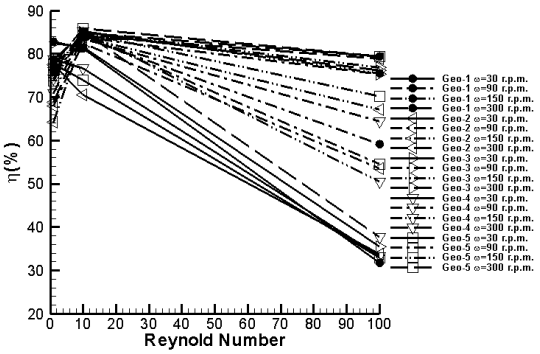

Fig. 14 A comparison of mixing efficiency at different rotation speeds

Appendix

NOMENCLATURE

A	=	the area of interlacing section
A_i	=	the area of ith ingredient on interlacing section
C_A	=	concentration of A
C_i	=	the mass fraction of ith ingredient
c_i	=	the concentration value of a certain grid
c_{max}	=	the maximum mixing concentration value
D	=	hydraulic diameter
E	=	eccentric moment (mm)
n	=	the number of grids for the concentration value on a certain cross-section
P	=	static pressure of flow (Pa)
R	=	generate radius (mm)
Re	=	Reynolds number, $\rho \bar{u} D/\mu$
$\bar{u}$	=	velocity vector
α	=	definition of mixing efficiency
Γ_A	=	molecule diffusion coefficient
η_N	=	numerical mixing efficiency
μ	=	viscosity of mixture
υ	=	kinematic viscosity
ρ	=	density of mixture
σ_{max}	=	the maximum change of mixing concentration value
ω	=	angular velocity (*r.p.m)*

References

[1] Yongdae Kim, Jongkwang Lee and Sejin Kwon, "A novel micro-mixer with a quasi-active rotor: fabrication and design improvement," *Journal of Micromechanics and Microengineering*, Vol. 19, No. 10, 105028, pp. 1-9, 2009 ◦

[2] Liu R. H., Stremler M.A., Sharp K. V., Olsen M. G., Santiago J. G., Adrian R. J., Aref H., and Beebe D. J., "Passive mixing in a three-dimensional serpentine microchannel," *J. Microelectromech. Sys.*, vol. 9, pp. 190-197, 2000 ◦

[3] N. T. Nguyen., and Z. Wu., "Micromixers: a Review," *Journal of Micromechanics and Microengineering*, Vol. 15, pp.1-16, 2005.

[4] Miyake R., Lammerink T. S. J., Elwenspoek M., and Fluitman J. H. J., "Micro mixer with fast diffusion," *Proc. MEMS'93, 6th IEEE Int. Workshop Micro Electromechanical System* (San Diego, CA), pp. 248-53, 1993 ◦

[5] Stroock, A. D., Dertinger, S. K., Ajdari, A., Stone, H. A., and Whitesides, G. M., "Chaotic mixer of microchannels," *Science*, 2002. 295: pp. 647-651 ◦

[6] Kim, D. S., Lee, S. W., Kwon, T. H., and Lee, S. S., "A barrier embedded chaotic mixer," *Journal of Micromech. Microeng.*, 2004. 14: pp. 798-805 ◦

[7] C. A. Cortes-Quiroz., A. Azarbadegan., and E. Moeendarbary., "An efficient passive planar micromixer with finshaped baffles in the tee channel for wide Reynolds number flow range,"*World Academy of Science, Engineering and Technology*, vol.61, pp. 170-175, 2010。
[8] Mubashshir Ahmad Ansari., Kwang-Yong Kim., Khalid Anwar., and Sun Min Kim., "A novel passive micromixer based on unbalanced splits and collisions of fluid streams," *Journal of Micromechanics and Microengineering*, Vol. 20, No.5, 005007, pp. 1-10, 2010.
[9] Ying Lin., Xinhai Yu., Zhenyu Wang., Shan-Tung Tu., and Zhengdong Wang., "Design and evaluation of an easily fabricated micromixer with three-dimensional periodic perturbation,"*Chemical Engineering Journal,* Vol. 171, Issue 1, pp. 291-300, 2011。
[10] Han E. H. Meijer, Mrityunjay K. Singh, Tae Gong Kang., Jaap M. J. Toonder., and Patrick D. Anderson., "Passive and Active Mixing in Microfludic device," *Macromolecular. Symposia.*, No. 279, pp. 201-209, 2009.
[11] Yang, Z., Goto, H., Matsumoto, M., and Yada, T., "Micromixer incorporated with piezoelectrially driven valveless micropump," *Micro Total Analysis Systems'98*, pp. 177-180, 1998.
[12] Yang, Z., Goto, H., Matsumoto, M., and Maeda, R., "Ultrasonic Micromixer for Microfluidic Systems," *MEMS 2000, The 13th Annual International Conference,* 2000.
[13] Li Kang-Hsis, "A Study of Active Micro-mixer Based on Pulsating Inlet Flows" *Master's thesis*, Tainan, Taiwan (2006).
[14] Shu Hao-Chieh, "Numerical Study of Mixing Enhancement with Time-Dependent Flowrate Modulation in Micromixers", *Master's thesis*, Taichung, Taiwan (2006)
[15] Chang Chih-Hsiang, Liu Da-Sheng, Kuo Lung-sheng, Chen Bing-hui, "The Improvement of the Mixing Efficiency of Semi-active Micro-mixers by Nano-magnetic Fluids", *the 24th National Colloquium held by Chinese Mechanical Engineering Association*, Chungli, Taoyuan, Taiwan, pp. 5148 – 5153.
[16] Wu Tzung-Hsin, Shao Yun-Lung, Huang Po-Cheng, Cheng Tsung-Chieh, "The Manufacture and Research of Micro-mixers", *Journal of Nano-communication*, Vol. 12, Issue 1, pp. 21-27.
[17] Jongkwnag Lee and Sejin Kwon., "Mixing efficiency of a multilamination micromixer with consecutive recirculation zones," *Journal of Chemical Engneering Science*, vol. 64, pp. 1223-1231, 2009。
[18] Lee, S. W., Kim, D. S., Lee, S. S., Kwon, T. H., "A split and recombination micromixer fabricated in a PDMS three-dimensional structure," *Journal of Micromechanics and Microengineering*, vol. 16, pp. 1067-1072, 2006。
[19] Hardt, S., Schönfeld, F., "Laminar mixing in different interdigital micromixers: II, Numerical simulation," *A.I.Ch.E. Journal,* vol. 49, pp. 578-584, 2003.
[20] Engler M., Kockmann N., Kiefer T., and Woias P., "Numerical and experimental investigations on liquid mixing in static micromixers," *Chemical Engineering Journal*, vol. 101, pp.315–322, 2004。

Jr-Ming Miao received his bachelor degree from Chung Cheng Institute of Technology in 1989 and Ph. D. degree from National Taiwan University in 1997. Afterwards, he joined the Dept. of Mechanical Engineering of Chung Cheng Institute of Technology as an associate professor. He was promoted to full professor in 2005. In August 2009, He transferred to National Pingtung University of Science and Technology to be a full professor and chairman of department of materials engineering. His research areas include CFD application on industry, micro-fluidics, PEMFC, MAV, low Reynolds number aerodynamics of flapping wing, and fluid-thermal process in cooling devices for electronic equipments, IPMC actuators.
E-mail: jmmiao@mail.npust.edu.tw